Macromolecules

ARTICLE

pubs.acs.org/Macromolecules

Heterogeneity in the Distribution of Entanglement Density during Polymerization in Disentangled Ultrahigh Molecular Weight Polyethylene

Anurag Pandey,[†,‡] Yohan Champouret,[†,‡] and Sanjay Rastogi*[,†,‡,§]

[†]Department of Materials, Loughborough University, Loughborough, LE11 3TU, U.K.

[‡]The Dutch Polymer Institute (DPI), P.O. Box 902, 5600 AX Eindhoven, The Netherlands

[§]Department of Chemical Engineering, Eindhoven University of Technology, P.O. Box 513, 5600 MB Eindhoven, The Netherlands

ABSTRACT: Ultrahigh molecular weight polyethylene is an engineering polymer that is widely used in demanding applications because of its unparallel properties such as high abrasion resistance, high-modulus and high-strength tapes and fibers, biaxial films, etc. In common practice, to achieve the uniaxial and the biaxial products, solution processing route is adopted to reduce the number of entanglement per chain. Another elegant route to reduce the number of entanglement is controlled polymerization using single-site catalytic system. In this publication, we address different polymerization conditions, temperature and time, to control molecular weight and the resultant entangled state. With the help of rheological studies, we show that heterogeneity in the distribution of entanglement along the chain during polymerization occurs. Because of living nature of the catalytic system, with increasing polymerization time molecular weight increases whereas the number of entanglement per unit chain decreases. These findings suggest that most of the entanglement is established at the initial stages of polymerization.

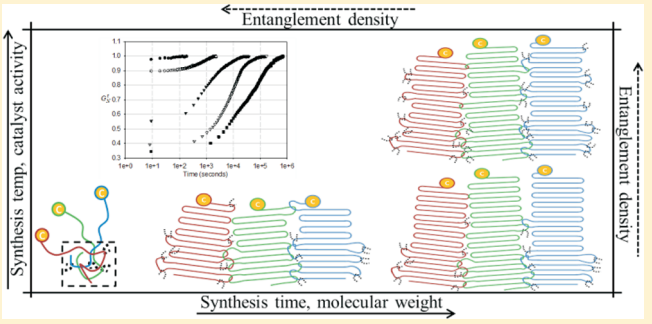

INTRODUCTION

The mechanical properties in polymers are strongly dependent on molecular characteristics. For example, in linear polyethylene, with increasing molecular weight from several hundred thousand g/mol to a million g/mol or above, mechanical properties such as tensile strength, modulus, and abrasion resistance increase to an extent that the polymer normally used for commodity applications becomes applicable for demanding applications, which include prostheses, lightweight strong fibers and tapes for ballistic applications, ropes for replacement of steel cables, etc. However, increased molecular weight of the polymers also adversely affects their processability, mainly due to the reduced number of chain ends and increased number of entanglement per chain. Thus, it has been always a quest to find balance between ease in processing and acquired mechanical properties.

Smith and Lemstra have shown improved processability of ultrahigh molecular weight polyethylene (UHMW-PE) by reducing the entanglement density by dissolution of the polymer (less than 5 wt %) in a solvent, such as decalin or xylene.[1,2] Later, Smith et al. also showed the possibility of synthesizing disentangled UHMW-PE under controlled synthesis conditions where polymerization temperature is decreased to an extent that the crystallization rate is favored over the polymerization rate, thus avoiding the entanglement formation.[3,4] For their studies the authors made use of supported vanadium catalyst, where the polymerization was performed below −20 °C. Because of low polymerization temperature, the polymer yield was sufficiently low; however, it was shown that the synthesized polymer can be compressed and drawn uniaxially to make fibres below the equilibrium melting temperature of linear polyethylene. Considerable studies have been performed to understand morphology developed during polymerization of the semicrystalline polymers, which are generally synthesized at a temperature below their melt-crystallization temperature.[4−19] Although most of these studies have been performed on samples synthesized using heterogeneous catalytic system, it is interesting to see the influence of polymerization conditions on the morphology of nascent crystals.

Normally in the commercially synthesized polymers, where the heterogeneous Z−N catalyst is used, the crystallization rate is slower than the polymerization rate. Moreover, in a heterogeneous catalytic system the active sites are tethered on a support and are close to each other, leading to a higher probability of finding the neighboring growing chains. This results in the entanglement formation during synthesis. In contrast to the heterogeneous synthesis, in the homogeneous synthesis catalyst and cocatalyst are dispersed in the polymerization medium. Thus, the homogeneous synthesis provides an opportunity to control the polymerization rate, crystallization rate, and desired separation

Received: February 17, 2011
Revised: April 21, 2011
Published: May 20, 2011

between the polymerization sites to tailor the entangled state of the synthesized polymer. Such a possibility results into the formation of disentangled polyethylene, ultimately resulting into a "single chain forming single crystal".[20−23]

Recently, in our group we made use of a single-site homogeneous catalytic system, and following the concept of single-site forming single crystal, we separated the active sites in the solvent to an extent that the growing chains do not overlap during polymerization at low polymerization temperature.[24] This novel synthesis also presents a possibility of synthesizing UHMW disentangled polymers with narrow polydispersity that could be deformed in the solid state to obtain high-modulus, high-strength tapes.[25] The synthesized UHMW-PE also provides an opportunity to investigate entanglement formation during polymerization and chain dynamics arising on melting of the disentangled crystalline state. Lippits et al. have studied the entanglement formation in such materials and have shown the effective use of rheology to follow the entanglement formation.[22,26]

In this work we have synthesized a series of UHMW-PE samples using a single site catalyst reported by Fujita and co-workers in dilute solution for different polymerization time and temperature.[27] The studies are performed to unravel the influence of polymerization conditions on the entanglement formation during polymerization. We also show suitability of melt rheology as a technique to measure the molecular weight (M_w) and molecular weight distribution (MWD) of UHMW-PE which has been demonstrated earlier by Talebi et al.[28] We use dynamic melt rheology to understand morphology produced during the synthesis and its effect on entanglement formation. Dynamic melt rheology is also used as a tool to investigate the entangled (or disentangled) state obtained on synthesis at different polymerization conditions.

Scheme 1. Ethylene Polymerization Using [3-*t*-Bu-2-O-$C_6H_3CH{=}N(C_6F_5)]_2TiCl_2$/MAO

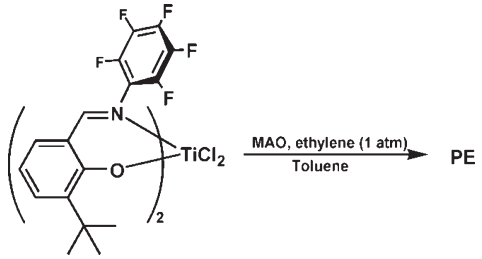

EXPERIMENTAL SECTION

1. Synthesis. *General.* All the manipulations of air and moisture-sensitive products are carried out under a dry nitrogen or argon atmosphere using drybox (MBraun Unilab) and/or standard Schlenk line techniques. The bis(phenoxyimine)titanium dichloride complex, [3-*t*-Bu-2-O-$C_6H_3CH{=}N(C_6F_5)]_2TiCl_2$, is purchased from MCAT and is used as received. MAO (10% weight in toluene) and dry toluene are used as received from Aldrich. All the other chemicals are commercially available and used as received. Ethylene (polymer grade) is purchased from BOC and used as received.

Ethylene Polymerization. All polymerizations are conducted using similar experimental conditions. A typical experiment is described here as a representative example. An oven-dried five-necked round-bottom flask equipped with a magnetic stirred bar, thermometer probe, and sintering cannula were previously dried under vacuum for 30 min and backfilled with nitrogen. Dried toluene is introduced to the reaction flask, followed by 1 mL of MAO, and nitrogen is bubbled through the solvent for 30 min under stirring. The nitrogen is then replaced by ethylene gas, which is left bubbling through the solvent. After 30 min, the desired amount of MAO (minus 2 mL) is introduced, and the reaction flask is then placed at the desired temperature. When the requisite temperature is reached, the polymerization is initiated by addition of the precatalyst [3-*t*-Bu-2-O-$C_6H_3CH{=}N(C_6F_5)]_2TiCl_2$ previously dissolved in 2 mL of toluene and activated by 1 mL of MAO solution. After the required polymerization time, the polymerization is quenched by addition of an acidified MeOH solution. The resulting polyethylene is filtered, washed with copious amounts of methanol/acetone, and dried overnight in a vacuum oven at 40 °C.

In this study, *N*-(3-*tert*-butylsalicylidene)-2,3,4,5,6-pentafluoroaniline[3-*t*-Bu-2-O-$C_6H_3CH{=}N(C_6F_5)]_2TiCl_2$ precatalyst has been used for the preparation of a range of UHMWPE. Typically, [3-*t*-Bu-2-O-$C_6H_3CH{=}N(C_6F_5)]_2TiCl_2$ is treated with 1100 equiv of MAO in toluene under an atmospheric pressure of ethylene with temperature and time being the only parameters that are variable during the polymerization reaction (Scheme 1 and Table 1).

From Figure 2, an increase in catalyst activity is noticeable from 10 to 30 °C, however, above 30 °C the catalytic activity decreases. The reason for the decrease in the activity, with increasing polymerization temperature, could be the same as mentioned above in the caption of Figure 1. In

Table 1. Different Polymerization Temperature and Time, Resulting in the Requisite Polymers[a]

sample	$[C_{Cat}]$ (mM)	toluene (L)	temp (°C)	time (min)	yield (g)	activity ($kg_{PE}\ mol_{cat}^{-1}\ h^{-1}$)	activity/[ethylene] ($kg_{PE}\ mol_{cat}^{-1}\ h^{-1}$) $(mol\ L^{-1})_{ethylene}$
dPE_10C_1′	0.012	1.5	10	1	3.1	10330	61 850
dPE_10C_2′	0.012	1.5	10	2	4.7	7830	46 890
dPE_10C_5′	0.012	0.5	10	5	4.1	6200	49 100
dPE_10C_10′	0.012	0.5	10	10	5.2	5200	31 140
dPE_10C_20′	0.012	0.5	10	20	10.1	5050	30 240
dPE_10C_30′	0.012	0.75	10	30	11.4	2530	15 150
dPE_20C_30′	0.012	0.75	20	30	23.9	5310	37 130
dPE_30C_30′	0.012	0.75	30	30	36.4	8090	65 240
dPE_40C_30′	0.012	0.75	40	30	22.1	4910	45 460
dPE_70C_30′	0.012	0.75	70	30	2.8	620	8 210

[a] Synthesis condition: cocatalyst = MAO (Al:Ti = 1100:1), ethylene pressure 1 atm, polymerization medium is toluene. After polymerization for the desired time the reaction is quenched with HCl/MeOH solution, and the polymer is filtered, washed, and dried in vacuum oven at 40 °C. The sample nomenclature reflects information on polymerization temperature and time, where time is measured immediately after addition of the activated catalytic system.

dx.doi.org/10.1021/ma2003689 |*Macromolecules* 2011, 44, 4952–4960

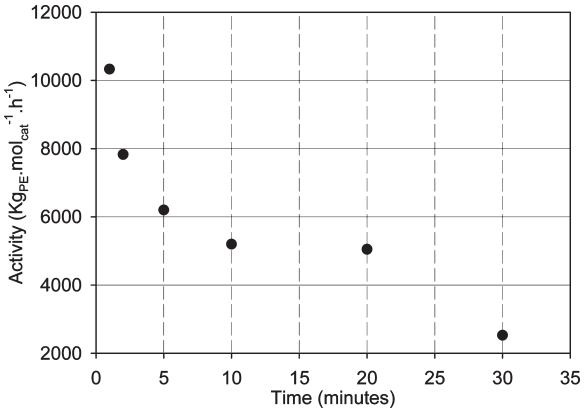

Figure 1. For the same polymerization temperature of 10 °C and polymerization conditions, activity of the catalyst, [3-*t*-Bu-2-O-C_6H_3CH═N-(C_6F_5)]$_2TiCl_2$/MAO, decreases with increasing polymerization time. The catalyst activity varies from 10 330 to 2530 kg mol^{-1} h^{-1} in toluene, as summarized in Table 1 and Figure 1. The decrease in activity could arise from heterogenization of the catalyst, increase in viscosity of the polymerization media due to precipitation of polymers, introduction of traces of catalyst poison with the ethylene feed, etc.

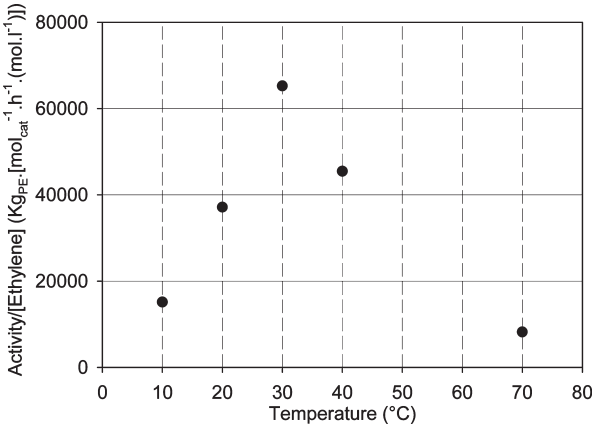

Figure 2. Catalyst activity/[ethylene][29,30] for ethylene polymerization using [3-*t*-Bu-2-O-C_6H_3CH═$N(C_6F_5)$]$_2TiCl_2$/MAO is performed at different temperatures for the same polymerization time, 30 min. The concentration of ethylene in toluene is calculated according to Henry's law: $\Phi_{ethylene} = p_{ethylene}H_0 \exp(\Delta H_L/RT)$ with $\Phi_{ethylene}$ = ethylene concentration (mol L^{-1}); $p_{ethylene}$ = ethylene pressure (atm); H_0 = Henry coefficient = 0.001 75 mol L^{-1} atm^{-1}; ΔH_L = enthalpy of solvation for ethylene in toluene = 2569 cal mol^{-1}; R = 1.989 cal mol^{-1} K^{-1}, and T = polymerization temperature (K).

addition to it, because of decrease in the solubility of ethylene with increasing temperature catalyst activity is also likely to decrease.[23,28] Furthermore, Fujita et al.[31] also suggested that chain termination or transfer and/or catalyst deactivation is not negligible at temperature above 50 °C.

2. Rheometry. *Sample Preparation for the Rheological Studies.* The nascent powder obtained from reactor is mixed with antioxidant (Irganox 1010), 0.7 wt %, to prevent any degradation over the long rheological experiments. To have homogeneous mixing of the antioxidant with the powder, the antioxidant is first dissolved in acetone and subsequently mixed with the nascent UHMWPE powder submerged in acetone. After mixing, the powder is dried overnight in vacuum oven at 40 °C. The dried powder is compressed into a plate of diameter 40−50 mm and thickness 0.6−0.7 mm at 125 °C, under the force of 20 tons

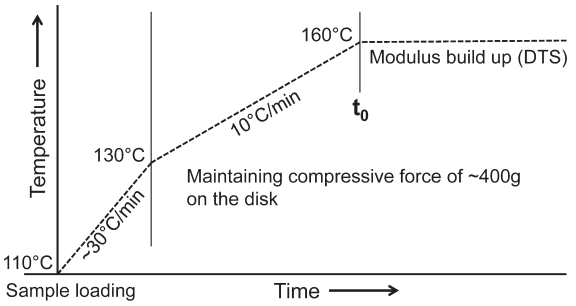

Figure 3. Schematic diagram for the rheological experiment protocol to follow modulus buildup (entanglement formation) at 160 °C for the samples synthesized at different polymerization time and temperature, as depicted in Table 1. Time t_0 in the figure represents start of the data collection after thermal stabilization, i.e., 100 s after reaching 160 °C.

for average time of 25 min. From the compressed plate several disks of 12 mm diameter are cut using a metal punch for rheology experiments.

Experimental Protocols for the Rheological Studies. All the rheological studies are performed on a strain-controlled rheometer, ARES, TA Instruments. In all rheological studies, a disk of 12 mm diameter is used to avoid excessive force to the rheometer transducers that the rubber-like melt state of the UHMWPE imposes. The disk between the parallel plates of the rheometer is heated to 110 °C under a nitrogen environment in a convection oven to prevent thermo-oxidative degradation. From 110 to 130 °C the sample is heated rapidly (∼30 °C/min). After waiting for the thermal stabilization at 130 °C (∼2 min), the sample is compressed with a compressive (normal) force of ∼400*g*. Autonormal force function, maintaining the constant force of ∼400*g*, is chosen throughout the experiment. The sample is heated at 10 °C/min from 130 to 160 °C. The dynamic amplitude sweep test is performed at a fixed frequency 100 rad/s to determine the linear viscoelastic regime. The dynamic time sweep test is performed to follow the entanglement formation at a fixed frequency of 10 rad/s and strain of 0.5% in the linear viscoelastic regime of the polymer.[22,23,26]

RESULTS AND DISCUSSION

To follow the influence of synthesis conditions on the entangled state, rheological studies are performed systematically on the synthesized polymers. All samples for the rheological studies are synthesized using the same catalytic system where the variable parameters during polymerization are time and temperature listed in Table 1. The two parameters are varied to understand the effect of time and temperature on the entanglement formation during synthesis.

1. Entanglement Formation in a Nascent Disentangled Polymer. Figure 4 shows dynamic time sweep data at 160 °C for the sample dPE_10C_5′, synthesized at 10 °C for 5 min. Data collection is started after thermal stabilization of the sample, i.e., after leaving the sample for 100 s at 160 °C, as depicted in Figure 3. Figure 4 shows that the elastic modulus (G') increases with the increasing annealing time at 160 °C. The elastic modulus for a thermodynamically stable polymer melt is related to average molecular weight between entanglement (or average entanglement density in melt) by the equation

$$G_N^0 = g_n \rho RT/M_e \quad (1)$$

where G_N^0 is the plateau modulus (in rubbery regime), g_n is a numerical factor (1 or 4/5 depending upon the convention), ρ is the melt density, R is the gas constant, T is the absolute temperature, and M_e is the molecular weight between entanglement.

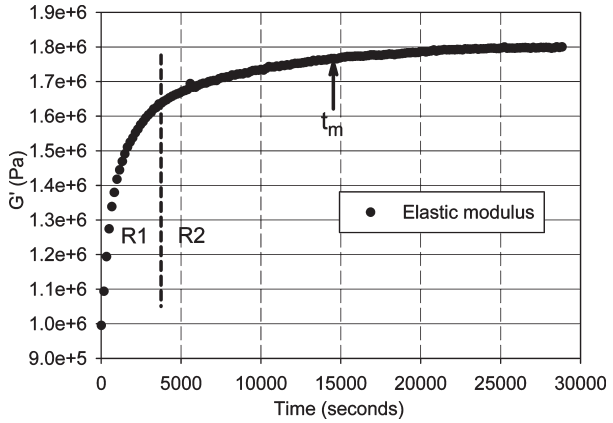

Figure 4. Dynamic time sweep test at 160 °C for disentangled sample dPE_10C_5′ at a constant frequency 10 rad/s and strain 0.5%. The modulus buildup with the increasing annealing time represents the increasing entanglement density (decreasing M_e) in the polymer melt (see eq 1). The modulus buildup is divided into two regimes, R1 and R2. Regime R1 is defined where 80% of the total modulus buildup occurs in 20% of the total entanglement time (t_m); the remainder of the modulus buildup in the 80% of the time is associated with the regime R2.

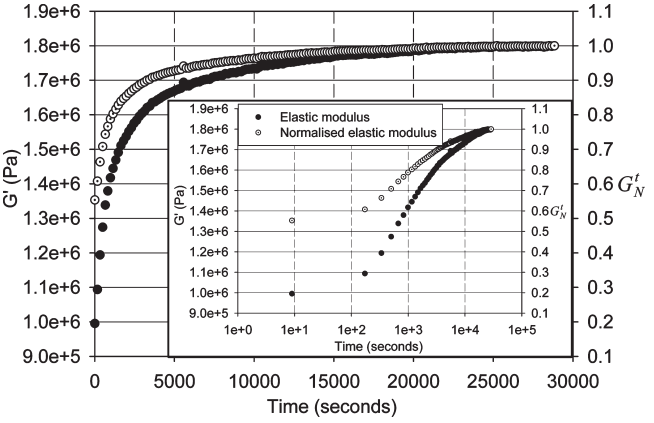

Figure 5. Absolute values of the elastic modulus (G') and the normalized elastic modulus (G_N^t) obtained on annealing the sample dPE_10C_5′ at 160 °C. Inset picture is the semilog plot of the same. Scaling for the *Y*-axis of G_N^t is chosen to show data points of the two moduli together.

Thus, in a melt state at a fixed temperature, the increasing elastic modulus relates to its increasing entanglement density, i.e., decrease of the average molecular weight between entanglement. From Figure 5, it is apparent that the initial modulus just after melting is ∼1 MPa. The modulus increases with time until it reaches to a maximum value of ∼1.8 MPa, G'_{max}, maximum plateau modulus value for a thermodynamically stable polyethylene melt. The time required for a disentangled polymer to reach 98% of its maximum plateau modulus is termed the total buildup time[22,23,26] (t_m) and is around 15 000 s for the sample dPE_10C_5′. Though eq 1 represents relationship between elastic modulus and molecular weight between entanglement in a thermodynamically stable state, for simplicity its application on the data shown in Figure 4 suggests varying molecular weight between entanglement with annealing time, i.e., a thermodynamically metastable melt state where rheological concepts for the thermodynamically stable melt state may not hold.

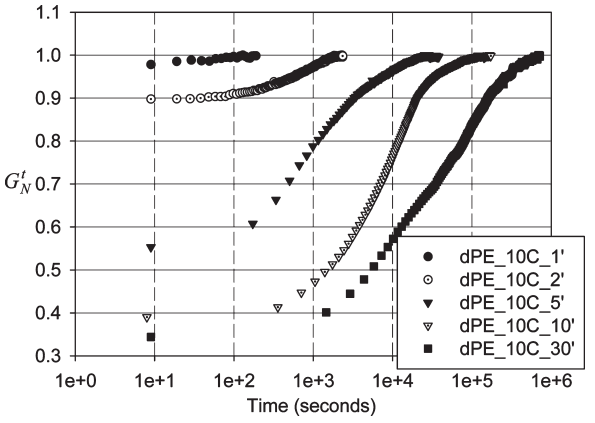

Figure 6. Dynamic time sweep at 160 °C for the samples synthesized at 10 °C for varying polymerization time. G_N^t is normalized elastic modulus, normalized by G'_{max} (maximum plateau modulus in the modulus buildup).

The two regimes illustrate differences in the rate of entanglement formation. In the regime R1 the rate of modulus buildup is faster and is associated with the entanglement formation by faster mixing of the polymer chains through the chain explosion process on melting.[32,33] However, in the regime R2, the entanglement formation is slower and predominantly governed by the reptation dynamics. After the modulus reaches to a plateau value of G'_{max} (1.8−1.9 MPa), the initially disentangled melt achieves the thermodynamic equilibrium and no further increase in the modulus occurs.

Figure 5 shows plot for the absolute values of elastic modulus along with the normalized elastic modulus (G_N^t). The modulus is normalized by the maximum plateau modulus (G'_{max}) in the modulus buildup and is given by

$$G_N^t = G'_t/G'_{max} \quad (2)$$

where G_N^t is the normalized elastic modulus at time t and G'_t is the absolute value of elastic modulus at variable time t. Data chosen are the same as shown in Figure 5. To accommodate long experimental time along the x-axis, the chosen graphic representation in the publication will be semilog as shown in the inset of Figure 5.

In a thermodynamically stable melt, chains acquire maximum number of entanglement at G'_{max}. Thus, at any given time t, G_N^t represents the number of entanglement present (entanglement density or M_e) and is a fraction of the total number of entanglement possible in a thermodynamically stable melt for a given molecular weight. Hence, we use G_N^t as a measure for fraction of the total number of entanglement present in a melt state at any given time t with respect to its thermodynamically stable state. The higher value of G_N^t reflects the higher entanglement density and lower molecular weight between entanglement (M_e). At unity, melt is thermodynamically stable and achieves maximum entanglement density, i.e., equilibrium entanglement molecular weight (∼1800 g/mol in case of PEs). Following these concepts, we address the entangled state of the synthesized polymer at different polymerization time and temperature.

2. Effect of Polymerization Time on Entanglement Formation. Figure 6 shows comparison of the normalized modulus buildup (G_N^t) on annealing at 160 °C for the samples synthesized at 10 °C for different polymerization time. The total entanglement time (t_m) increases with the increasing polymerization

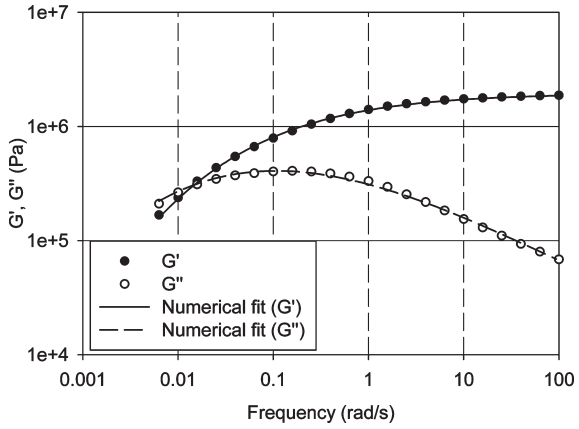

Figure 7. An example of dynamic frequency sweep data (performed on a sample dPE_10C_5′ at 160 °C and constant strain 0.5%) along with the numeric fit to obtain M_w and MWD. For the numerical fit the Orchestrator software's in-built analysis tool is used.

time. For example, to reach the maximum modulus it takes about 1000 s in the sample synthesized for 2 min compared to a week required for the modulus buildup in the sample synthesized for 30 min. Consistent decrease in the normalized modulus at t_0 suggests decreasing density of entanglement in the nascent polymer with increasing polymerization time.

For a pure living catalytic system, molecular weight increases linearly with the polymerization time. For a thermodynamically stable melt, the number of entanglement per chain increases with increasing molecular weight as equilibrium entanglement molecular weight (M_e) is considered to be intrinsic for a given polymer. Hence, higher molecular weight sample will require more time to reach the thermodynamically stable state from its disentangled state.

To have molecular insight on the synthesized polymer, it is of utmost importance to determine molecular weight and molecular weight distribution. For the purpose molecular rheology is applied as a tool described in the following section.

3. M_w and MWD Determination Using Dynamic Melt Rheology. Using a standard GPC technique, it is not easy to determine the molecular weight (M_w) and molecular weight distribution (MWD) of polyethylene exceeding the molecular weight, M_w > 1 million g/mol.[28] Following the methods described by Mead[34] and Tuminello,[35] from dynamic melt rheology, M_w and MWD data can be numerically synthesized. Viscosity model and modulus model are generally used to numerically synthesize the M_w and MWD from the melt rheology data. In viscosity model the M_w and MWD are computed from the rheological behavior of the material's viscosity dependence on the shear rate.[36,37] However, the modulus model describes viscoelastic properties for polymers with high molecular weight components and is more suitable for high M_w polymers synthesized in this study. The modulus model is presented in terms of relaxation modulus which takes relaxation spectrum from time domain of the material and converts it into molecular weight domain.[28] The MWD curve is then obtained through regularized integral inversion.

One the most successful algorithms in predicting the molecular weight distribution of a nearly monodisperse, broad and bimodal polymer melt is developed by Mead.[34] This algorithm has been commercialized by Rheometric Scientific for incorporation in their Orchestrator software and used here for the determination of M_w and MWD. Tuminello[35] and Talebi et al.[28] have shown usability of the technique to determine M_w and MWD on a series of polymers having molecular weight ranging between 35 000 and 10 million g/mol. A dynamic frequency sweep within the linear regime, at 160 °C, is performed on a thermodynamically stable melt obtained after reaching the G'_{max}. This is considered to be the requisite as all theoretical models are applicable on the thermodynamically stable melt state.

Table 2. M_w and MWD along with the Total Entanglement Buildup Time, t_m, for Samples Synthesised at 10 °C for Varying Polymerization Time

samples	M_w (million g/mol)	MWD	total entanglement time, t_m (s)
dPE_10C_1′	0.3	1.4	20
dPE_10C_2′	0.6	1.7	1 220
dPE_10C_5′	1.4	2.5	14 260
dPE_10C_10′	2.5	2.4	64 640
dPE_10C_20′	3.7	2.8	120 500
dPE_10C_30′	5.1	2.5	423 430

The numerical fit of molecular weight and molecular weight distribution to the dynamic frequency sweep data at 160 °C for sample dPE_10C_5′ is shown in Figure 7. A numerically synthesized MWD curve for such a fit is shown in Figure 8b along with the other samples synthesized for different polymerization times. Thus, determined M_w and MWD of the synthesized samples are summarized in Table 2. From the data it is evident that molecular weight increases with the increasing polymerization time; however, the increase is not linear (Figure 8a) as the catalyst activity decreases with the increasing time (see Figure 1).

Figure 6 shows that the total entanglement buildup time, t_m, increases with the increasing molecular weight and has been tabulated in Table 2. The total entanglement time scales with the power of ∼2.6 to the molecular weight (see Figure 9). The lower scaling of ∼2.6 compared to the ∼3.0 in reptation time (of UHMWPE) in a thermodynamically stable melt can be associated with (a) faster entanglement formation due to physical mixing process immediately after melting of the disentangled crystals and (b) faster reptation dynamic arising in the initially "disentangled" melt state having lesser number of entanglement. Similar lower scaling of total entanglement time to the molecular weight has been reported in the earlier work.[22,23]

4. Effect of Polymerization Time on Entangled State of the Nascent Polymer. In Figure 7, it can be seen that G_N^t at time t_0 decreases with the increasing molecular weight. For $t = 0$ eq 2 can be modified as

$$G_N^{t=0} = G'_{t=0}/G'_{max} \quad (3)$$

where $G_N^{t=0}$ is the normalized elastic modulus at time t_0 and $G'_{t=0}$ is the absolute value of elastic modulus at time t_0.

$G_N^{t=0}$ gives an estimate of entanglement density at time t_0 which represents fraction of the total entanglement present in a nascent polymer immediately after melting. Some entanglement formation in the process of heating from 140 to 160 °C cannot be ignored. However, compared to the time required for the complete modulus buildup that exceeds for several hours depending on the molecular weight, hundreds of seconds lost in the process of heating above the equilibrium melting point and temperature stabilization are relatively small. In Figure 10, $G_N^{t=0}$ can be seen decreasing with the increasing molecular weight. It is counterintuitive to see that the higher molecular weight nascent samples have lower en-

dx.doi.org/10.1021/ma2003689 |Macromolecules 2011, 44, 4952–4960

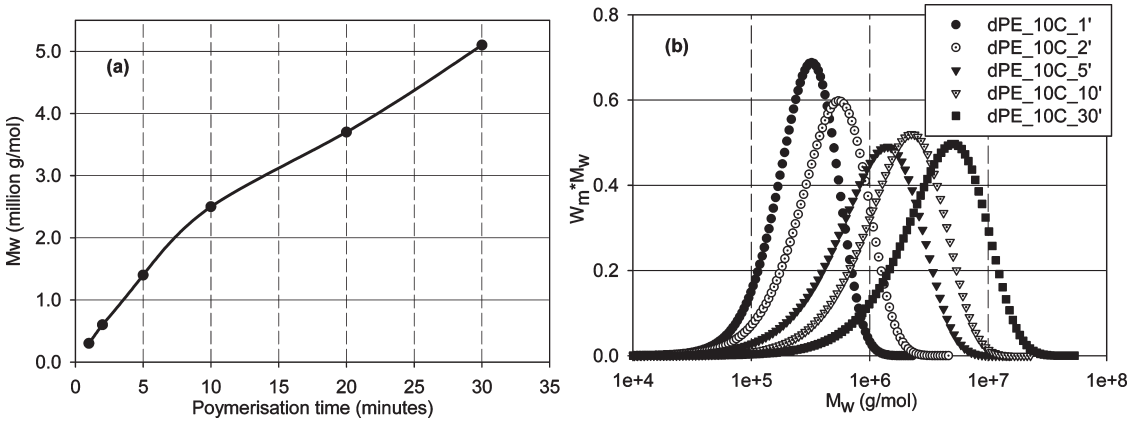

Figure 8. Numerically synthesized (a) M_w and (b) MWD curves using Orchestrator software's in-built analysis for M_w and MWD determination for a series of samples synthesized for different polymerization time listed in Table 2.

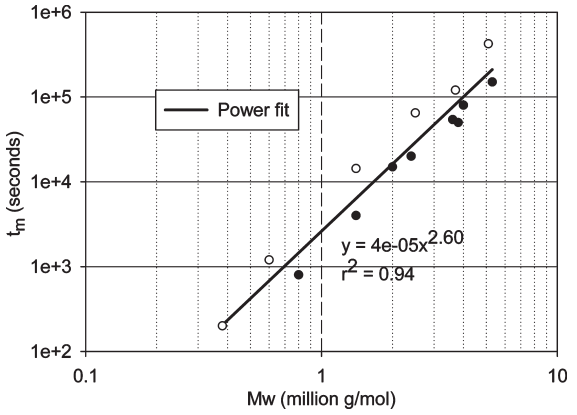

Figure 9. Total entanglement time (t_m) for different molecular weights. The total entanglement time scales t_m with the power of ~2.6 with the molecular weight. These observations are in accordance with the earlier data reported by Lippits[22] and Talebi.[23] Open symbols are data obtained from the study in this publication, whereas the filled symbols are data composed from previous studies.

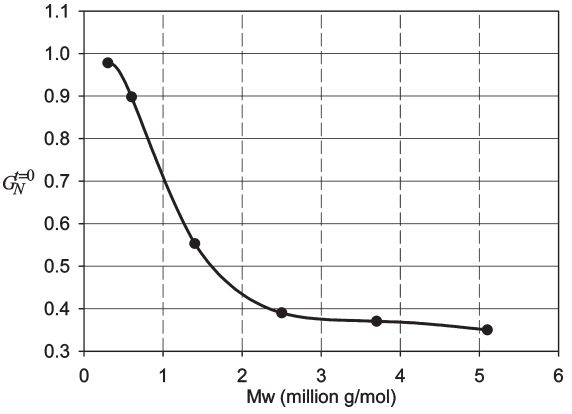

Figure 10. Storage modulus immediately after melting of samples having different molecular weight. The modulus represents inverse of molecular weight between entanglement.

tanglement density (higher M_e) compared to the lower molecular weight nascent samples of similar MWD.

The novel synthesis of the disentangled polymers is based on the conditions where the catalyst concentration is so low that growing chains from their single-site catalyst do not see each other and hence present lesser probability for overlapping of the growing chains to avoid entanglement formation.[3,4,20−23] Another important factor in the synthesis of disentangled polymers is the lower polymerization temperature than the crystallization temperature; thus, polymerization and crystallization kinetics will have a strong influence on the resulting entangled state of the nascent polymer. For example, the polymerization temperature determines the catalyst activity (rate of polymerization) and also the crystallization rate of the growing chains. At higher polymerization temperature catalyst activity normally increases, causing an increase in the polymerization rate. However, at the same time the increased temperature also causes decrease in crystallization rate of the growing chains. It is anticipated that faster crystallization rate would suppress overlapping of chains and would result into lesser entangled nascent state. Thus, the resultant entangled state is the balance between the rate of polymerization and crystallization that determines the entanglement density arising at a polymerization condition. From Figure 1 it is apparent that the catalyst activity decreases substantially after 5−10 min of polymerization. The decrease in catalyst activity, i.e., polymerization rate, will favor the lesser entanglement formation as the crystallization rate at the fixed temperature will remain the same. In this respect the observed decrease in $G_N^{t=0}$ (i.e., decreasing entanglement density) depicted in Figure 10, with increasing molecular weight (i.e., with increasing polymerization time) is in accordance with the decreasing catalyst activity shown in Figure 1.

Although the reactor bath for polymerization is maintained at 10 °C, it does not imply that the temperature achieved at the very local site of the catalyst where polymer chain is growing will be the same. In very early stages of polymerization, i.e., immediately after injection of the catalytic system in the ethylene saturated solvent, the local temperature at the catalyst site can be much higher than the desired polymerization temperature due to heat release on polymerization and crystallization. However, as the time lapses with polymerization, the local and global temperature of reaction equilibrates to the set polymerization temperature. At a fixed temperature, the crystallization rate of the growing chains also starts increasing over the polymerization rate due to the decreasing catalyst activity that may arise due to difficulty in ethylene diffusion to the active site. The gradual decrease in the

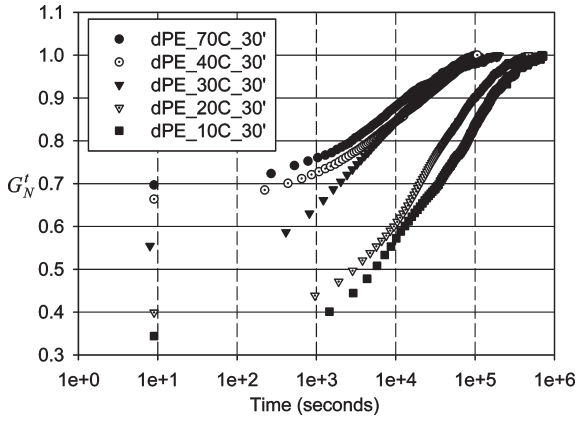

Figure 11. Normalized elastic modulus for dynamic time sweep at 160 °C for different polymer samples synthesized at different polymerization temperature. It can be seen that starting value of G_N^t at t_0 decreases for the polymer samples synthesized at lower temperatures.

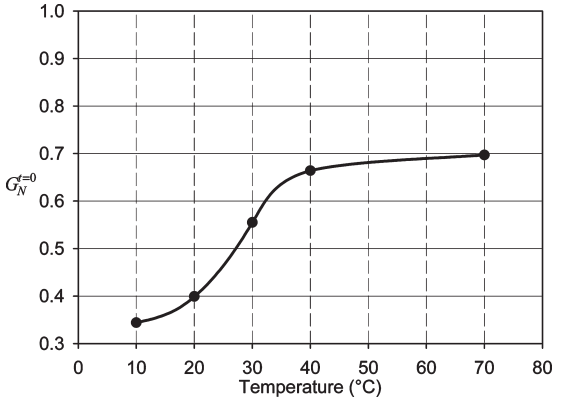

Figure 12. Entanglement density present in the nascent disentangled samples synthesized at different temperature immediately after melting.

polymerization rate while keeping the crystallization rate same, at a fixed temperature with increasing time, leads to lesser probability of entanglement formation.

The higher value of $G_N^{t=0}$ for lower molecular weight samples highlights the fact that the entanglement density is higher in these samples than the high molecular weight samples synthesized for longer polymerization time. Higher entanglement density in low molecular weight samples is caused by higher probability of the entanglement formation due to the higher catalyst activity and higher temperature at local site of the catalyst in the initial stages of polymerization. With increasing polymerization time, the catalyst activity slows down effectively and crystallization of the growing chains increases as the polymer chains grow. This leads to a scenario where one end of the chain has higher entanglement density (lower M_e) compared to the other end which has grown at the later stages of polymerization, causing a heterogeneous distribution of the entanglement density in the amorphous region of the crystal. On melting of the nascent disentangled polymers, having heterogeneity in the distribution of entanglement, the heterogeneity is slowly lost because of physical mixing and reptation dynamics as chains approach toward thermodynamically stable melt state (homogeneous melt). The average molecular weight between entanglement is higher in the higher molecular weight nascent disentangled samples compared to the lower molecular weight samples. The entanglement density produced during the polymerization can also depend upon several parameters such as the polymerization temperature, catalyst activity, heat and mass transfer within the bulk of reaction, solubility of ethylene in the solvent used, etc. What follows are the observations on the samples synthesized at higher temperatures while keeping the same polymerization time and other synthesis conditions.

5. Effect of Polymerization Temperature on Entanglement Molecular Weight. In the section above we hypothesized that during polymerization, especially at the initial stages, temperature at local catalyst site may increase the entanglement formation. To recall, entanglement density decreases with increasing polymerization time or increasing molecular weight. To have further insight into the influence of polymerization temperature on the entanglement formation, polymerization temperature is varied while maintaining the same polymerization time and other polymerization conditions (solvent, pressure, catalyst concentration, etc.). The effect of

Table 3. M_w and MWD of Samples Synthesised at Different Temperature for a Fixed Polymerization Time of 30 min[a]

samples	M_w (million g/mol)	MWD	total entanglement time, t_m (s)
dPE_10C_30′	5.1	2.5	423 430
dPE_20C_30′	6.3	2.4	266 310
dPE_30C_30′	4.7	2.9	88 450
dPE_40C_30′	5.2	3.1	72 270
dPE_70C_30′			62 470

[a] Due to extremely broad molecular weight distribution of the sample dPE_70C_30′, it was not possible to determine the trusted molecular weight and molecular weight distribution.

polymerization temperature on the rate of entanglement formation is shown in Figure 11, where entanglement formation occurs faster in samples synthesized at higher temperatures. Figure 12 depicts that the samples synthesized at higher temperatures have higher $G_N^{t=0}$ and thus higher entanglement density. The presence of high entanglement density in the nascent polymer also promotes the faster entanglement formation on melting and subsequently reduces the total entanglement time. The M_w and MWD of the samples along with their total entanglement buildup time are tabulated in Table 3. From the Table 3 and Figure 12 it is apparent that though the samples dPE_10C_30′ and dPE_40C_30′ have similar molecular weight and molecular weight distribution, the time required for the modulus buildup of the sample dPE_10C_30′ is much larger than the sample dPE_40C_30′. The distinction in the modulus buildup time is attributed to the higher initial entangled state ingrained in the sample dPE_40C_30′ due to its higher polymerization temperature. It is also to be realized that the modulus buildup time, entanglement formation, in these samples is also coupled by factors such as MWD, the entanglement density present due to different crystallization rate and catalyst activity (Figure 2) at different polymerization temperature.

From Figure 12, it is apparent that $G_N^{t=0}$ increases with increasing polymerization temperature and becomes almost constant at higher polymerization temperature. Though the reduction in catalyst activity above 30 °C (Figure 2) will favor the disentangled state; however, at the same time reduced crystallization rate at the higher temperature will favor the entanglement formation. Thus, the net effect of increasing polymerization temperature, above 30 °C, on the change in entanglement density is negligible.

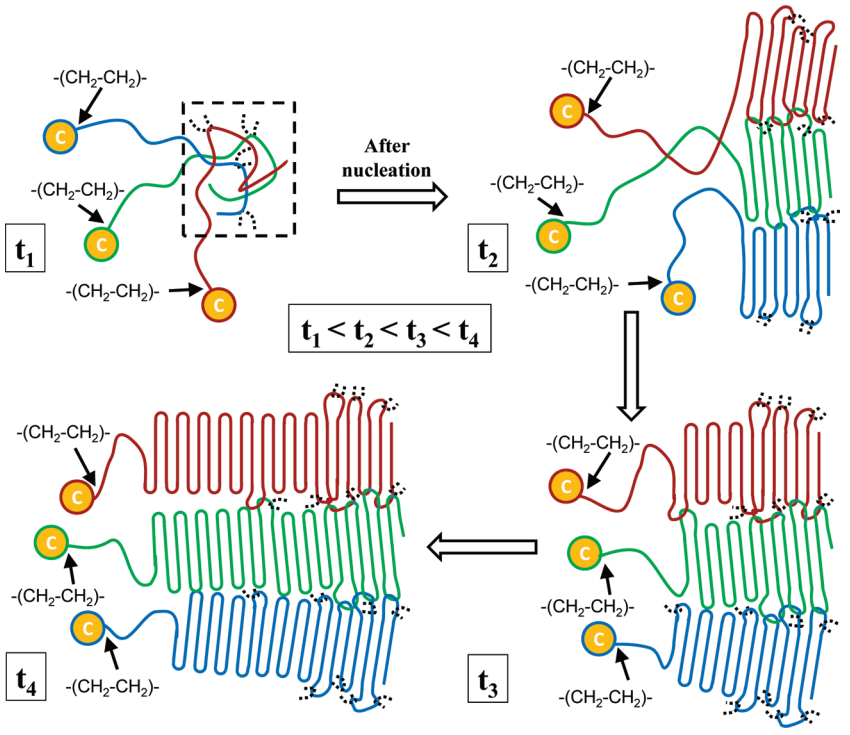

Figure 13. Schematic drawing showing chain growth from three different catalytic sites, where entanglement are realized at the initial stages prior to crystallization. Dotted black loops represent entanglement formation from the neighboring chains other than polymer chains represented by red—blue—green. Discontinuous rectangular box represents entanglement formation prior to crystallization thus nucleation process will lead to the entangled crystallized state at time t_2. Once the nucleus is formed, at a distance from the exothermic polymerization catalytic site, with the suppression of the nucleation barrier crystal growth will be substantially enhanced, depicted for time t_3. With the polymer crystal formation in the surrounding of the catalyst, ethylene diffusion will decrease continuously and reduce the polymerization kinetics. The reduction in polymerization kinetics combined with suppressed nucleation barrier will strongly favor crystallization of the growing chains and formation of the disentangled polyethylene with increasing molecular weight, the situation depicted for time t_4.

In addition to the concepts summarized above on the entanglement formation with polymerization time and polymerization temperature, crystallization at the later stages of polymerization time will be also favored due to suppression in the nucleation barrier, once the crystal is nucleated due to the growing chain.

CONCLUSIONS

In this publication we have conclusively shown rheology as an effective experimental tool to qualitatively assess the entangled state in the synthesized nascent polymer. Experimental observations are that in the early stages of polymerization the number of entanglement formed will be higher, where the number of entanglement tends to decrease with increasing polymerization time and the resultant molecular weight. The decrease in entanglement density with increasing molecular weight (or polymerization time) is explained because of the favored crystallization rate over the polymerization rate. For the same polymerization conditions, with time the crystallization rate is anticipated to gain an upper hand over the polymerization rate because of the (a) suppression in nucleation barrier due to crystallization of chains synthesized at the earlier stages, (b) decrease in catalyst activity due to difficulty in diffusion of ethylene to the active center, (c) and decrease in the temperature difference at the catalyst and its surroundings due to exothermic polymerization. These concepts are further strengthened by experiments performed at different polymerization temperature where the entanglement density is higher for higher polymerization temperature. These concepts are depicted in a schematic drawing shown in Figure 13.

The figure shows, prior to crystallization as the chains grow in their length, they will have strong probability to find each other and entangle, time t_1. (Even in very dilute catalytic concentration, if the chains will not find each other, they will have the tendency to form intramolecular entanglement, prior to nucleation.) Further at time t_2, considering polymerization to be exothermic process, at a distance from the catalytic site temperature would be lower and chains will tend to crystallize. The crystallization (or nucleation at this stage) will push entanglement in the amorphous region. At the depicted time t_3, the crystallized domains will suppress the nucleation barrier and the growing chains from the same catalytic site will crystallize faster. With increasing polymerization time, t_4, as the catalyst will be surrounded more and more from the crystallized polymer, ethylene diffusion will become difficult thus the polymerization rate will decrease constantly giving the upper hand to the crystallization of the growing chains. This process in single site catalytic system would ultimately favor the formation of disentangled polyethylene with increasing molecular weight, i.e., reduction of entanglement density with increasing chain length. In the follow-up publications we will show the influence of reduced entanglement in the ease in solid state processing of the polymers having weight-average molecular weight exceeding above 4 million g/mol.

AUTHOR INFORMATION

Corresponding Author

*Tel: +44 (0) 1509 223156. Fax: +44 (0) 1509 223949. E-mail: s.rastogi@lboro.ac.uk.

■ ACKNOWLEDGMENT

This work is part of the Research Programme of the Dutch Polymer Institute (DPI), Eindhoven, The Netherlands, Project No. #637. We are thankful to Dr. Sara Ronca and Mr Giuseppe Forte for useful discussions.

■ REFERENCES

(1) Smith, P.; Lemstra, P. J. *Macromol. Chem.* **1979**, *180*, 2983–2986.
(2) Smith, P.; Lemstra, P. J. *J. Mater. Sci.* **1980**, *15*, 505–514.
(3) Smith, P.; Chanzy, H. D.; Rotzinger, B. P. *Polym. Commun.* **1985**, *26*, 258–260.
(4) Smith, P.; Chanzy, H. D.; Rotzinger, B. P. *J. Mater. Sci.* **1987**, *22*, 523–531.
(5) Blais, P.; Manley, R. St. J. *J. Polym. Sci., Part A-1* **1968**, *6*, 291–334.
(6) Keller, A.; Willmouth, F. M. *Macromol. Chem.* **1969**, *121*, 42–50.
(7) Graff, R. J. L.; Kortleve, G.; Vonk, C. G. *Polym. Sci. Polym. Lett.* **1970**, *8*, 735–739.
(8) Chanzy, H. D.; Revol, J. F.; Marchessault, R. H.; Lamande, A. *Kolloid Z. Z. Polym.* **1973**, *251*, 563–576.
(9) Munoz-Escalona, A.; Parada, A. *J. Cryst. Growth* **1980**, *48*, 250–258.
(10) Kakugo, M.; Sadatoshi, H.; Yokoyama, M.; Kojima, K. *Macromolecules* **1989**, *22*, 547–551.
(11) Kakugo, M.; Sadatoshi, H.; Sakai, J.; Yokoyama, M. *Macromolecules* **1989**, *22*, 3172–3177.
(12) Tervoort-Engelen, Y. M. T.; Lemstra, P. J. *Polym. Commun.* **1991**, *32*, 343–345.
(13) Nooijen, G. A. H. *Eur. Polym. J.* **1994**, *30*, 11–15.
(14) Uehara, H.; Nakae, M.; Kanamoto, T.; Ohtsu, O.; Sano, A.; Matsuura, K. *Polymer* **1998**, *39*, 6127–6135.
(15) Ivan'kova, E. M.; Myasnikova, L. P.; Marikhin, V. A.; Baulin, A. A.; Volchek, B. Z. *J. Macromol. Sci., Part B: Phys.* **2001**, *B40*, 813–832.
(16) Uehara, H.; Aoike, T.; Yamanobe, T.; Komoto, T. *Macromolecules* **2002**, *35*, 2640–2647.
(17) Tsobkallo, K.; Vasilieva, V.; Khizhnyak, S.; Pakhomov, P.; Galitsyn, V.; Ruhl, E.; Egorov, V.; Tshmel, A. *Polymer* **2003**, *44*, 1613–1618.
(18) Tsobkallo, K.; Vasilieva, V.; Kakiage, M.; Uehara, H.; Tshmel, A. *J. Macromol. Sci., Part B: Phys.* **2006**, *45*, 407–415.
(19) Uehara, H.; Uehara, A.; Kakiage, M.; Takahashi, H.; Murakami, S.; Yamanobe, T.; Komoto, T. *Polymer* **2007**, *48*, 4547–4557.
(20) Gruter, G. J. M.; Wang, B. EP 1057837, DSM N.V. The Netherlands, 2000.
(21) Sharma, G. K. Easily processable ultra high molecular weight polyethylene with narrow molecular weight distribution. Ph.D. Thesis, Eindhoven University of Technology, 2005.
(22) Lippits, D. R. Controlling the melting kinetics of polymers; a route to a new melt state. Ph.D. Thesis, Eindhoven University of Technology, 2007.
(23) Talebi, S. Disentangled polyethylene with sharp molar mass distribution; Implications for sintering. PhD Thesis, Eindhoven University of Technology, 2008.
(24) Rastogi, S.; Garkhali, K.; Duchateau, R.; Gruter, G. J. M.; Lippits, D. R. US 7671159 B2, 2010.
(25) De Weijer, A. P.; Van De Hee, H.; Peters, M. W. M. G.; Rastogi, S. WO/2009/007045A1, 2009.
(26) Lippits, D. R.; Rastogi, S.; Talebi, S.; Bailly, C. *Macromolecules* **2006**, *39*, 8882–8885.
(27) Mitani, M.; Furuyama, R.; Mohri, J.-I.; Saito, J.; Ishii, S.; Terao, H.; Kashiwa, N.; Fujita, T. *J. Am. Chem. Soc.* **2002**, *124*, 7888–7889.
(28) Talebi, S.; Duchateau, R.; Rastogi, S.; Kaschta, J.; Peters, G. W. M.; Lemstra, P. J. *Macromolecules* **2010**, *43*, 2780–2788.
(29) Tritto, I.; Marestin, C.; Boggioni, L.; Sacchi, M. C.; Brintzinger, H. H.; Ferro, D. R. *Macromolecules* **2001**, *34*, 5770–5777.
(30) Yang, H.; Wang, Q.; Fan, Z.; Xu, H. *Polym. Int.* **2004**, *53*, 37–40.
(31) Mitani, M.; Mohri, J. I.; Yoshida, Y.; Saito, J.; Ishii, S.; Tsuru, K.; Matsui, S.; Furuyama, R.; Nakano, T.; Tanaka, H.; Kojoh, S. I.; Matsugi, T.; Kashiwa, N.; Fujita, T. *J. Am. Chem. Soc.* **2002**, *124*, 3327–3336.
(32) Barham, P.; Sadler, D. M. *Polymer* **1991**, *32*, 393–395.
(33) Rastogi, S.; Lippits, D. R.; Peters, G. W. M.; Graf, R.; Yao, Y.; Spiess, H. W. *Nature Mater.* **2005**, *4*, 635–641.
(34) Mead, D. W. *J. Rheol.* **1994**, *38*, 1797–1827.
(35) Tuminello, W. H. *Polym. Eng. Sci.* **1986**, *26*, 1339–1347.
(36) Bersted, B. H. *J. Appl. Polym. Sci.* **1975**, *19*, 2167–2177.
(37) Bersted, B. H.; Slee, J. D. *J. Appl. Polym. Sci.* **1977**, *21*, 2631–2644.